https://doi.org/10.5194/egusphere-2023-1115
Preprint. Discussion started: 29 June 2023

Differentiating between crop and soil effects on soil moisture dynamics

Helen Scholz[1], Gunnar Lischeid[2,3], Lars Ribbe[1], Kathrin Grahmann[2],

[1]Institute for Technology and Resources Management in the Tropics and Subtropics (ITT), TH Köln, Cologne, Germany
[2]Leibniz Centre for Agricultural Landscape Research (ZALF), Müncheberg, Germany
[3]Institute for Environmental Sciences and Geography, University of Potsdam, Potsdam, Germany

Correspondence to: kathrin.grahmann@zalf.de

Abstract. There is urgent need for developing sustainable agricultural land use schemes. On the one side, climate change is expected to increase drought risk as well as the frequency of extreme precipitation events in many regions. On the other side crop production has induced increased greenhouse gas emissions and enhanced nutrient and pesticide leaching to groundwater and receiving streams. Consequently, sustainable management schemes require sound knowledge of site-specific soil hydrological processes, accounting explicitly for the interplay between soil heterogeneities and crops. Here we present a powerful diagnostic tool applied to a highly diversified arable field with seven different crops and two management schemes. A principal component analysis was applied to a set of 64 soil moisture time series.

About 97% of the spatial and temporal variance of the data set was explained by the first five principal components. Meteorological drivers accounted for 72% of the variance. Another 17% was attributed to different seasonal behaviour of different crops. The effect of very low soil moisture in deeper layers at the onset of the growing season explained another 4.1%, and soil texture 2.2%. The fifth component represented the effect of soil depth (1.7%). In contrast, neither topography nor weed control had a significant effect on soil moisture. Contrary to common expectations, soil and rooting pattern heterogeneity seemed not to play a major role in this case study.

1 Introduction

Agriculture plays a major role to ensure food for a growing global population. At the same time, climate change is putting yield stability at risk due to extreme weather events and is increasing the need for sustainable management of resources, such as water and soil (Trnka et al., 2014). As part of the adaptation to more challenging conditions, the transformation from large homogeneously cropped fields towards diversified agricultural landscape was identified not only to have positive effects on multiple ecosystem services (Tamburini et al., 2020), but also on the system's resilience to climatic extremes (Birthal and Hazrana, 2019). Additionally, crop diversification is highly beneficial by reducing soil erosion through permanent soil cover (Paroda et al., 2015), and by improving resource use efficiency through wider crop rotations (Rodriguez et al., 2021). In terms of soil water dynamics, diversification can lead to improved water-stable macro-aggregation, reduced soil compaction and

https://doi.org/10.5194/egusphere-2023-1115
Preprint. Discussion started: 29 June 2023

increased soil organic carbon (Karlen et al., 2006) from which soil water infiltration and retention can be positively affected (Alhameid et al., 2020).

However, as the complexity of the system increases due to diversification measures, so does the complexity of the assessment and monitoring what makes the use of digital technologies indispensable. Therefore, soil sensing networks received much attention as a crucial tool in Precision Agriculture (PA) (Salam and Raza, 2020). The main goal of PA is to increase efficiency and productivity at the farm level and at the same time minimizing negative impacts on the environment (Taylor and Whelan, 2010). Soil sensor networks play a vital role in achieving that and are used for various purposes, such as for supporting the delineation of management zones (Khan et al., 2020; Salam and Raza, 2020). One of the most important demands to be fulfilled by soil sensing networks, however, is soil moisture monitoring. Accurate measurement of soil water content will play an important role in improving crop yields and water management (Salam, 2020).

Wireless solutions, for instance based on LoRaWAN (Long Range Wide Area Network) technology, in combination with Time-Domain-Reflectometry (TDR) sensors avoid labour-intensive and destructive soil moisture measurements that disrupt field traffic. The development of such wireless soil monitoring networks enables broad and affordable application also in areas with low cellular coverage (Cardell-Oliver et al., 2019; Lloret et al., 2021; Placidi et al., 2021; Prakosa et al., 2021).

The evolvement of such systems does not only have benefits for management but is also of high relevance for fostering the understanding of hydrological dynamics in the vadose zone. High-resolution datasets measured under real farming conditions can be used to characterize and analyse spatio-temporal dynamics of soil water. Due to the large size of data sets that are recorded with novel sensor networks, sophisticated data analysis approaches are required to detect hidden patterns and determine influence factors on soil moisture variability (Vereecken et al., 2014). Methods include geostatistical analysis approaches, such as soil moisture variograms (Vereecken et al., 2014). With the introduction of multiple-points geostatistics, it became possible to not only analyse patterns but also connect them with factors affecting soil moisture, such as topography, texture, crop growth and water uptake, and land management (Brocca et al., 2010; Strebelle et al., 2003). Wavelet analysis can analyse both localized features as well as spatial trends through which non-stationary variation of soil properties can be considered (Si, 2008). Cross-correlation analysis allowed linking soil moisture variability to climatic variables (Mahmood et al., 2012). Furthermore, temporal stability analyses detect spots in the investigated area which are consistently wetter or drier than the mean soil moisture (Baroni et al., 2013). This method was already successfully used to detect soil moisture patterns related to soil properties, vegetation, and topography (Zhao et al., 2010).

Principal component analysis (PCA) is another method that was successfully applied for soil moisture variability analysis at the field (Hohenbrink et al., 2016; Hohenbrink and Lischeid, 2015; Martini et al., 2017), catchment (Korres et al., 2010; Lischeid et al., 2017; Nied et al., 2013), and regional (Joshi and Mohanty, 2010) scale. These studies build on previous applications in climatology where the term “Empirical Orthogonal Functions” is used (Bretherton et al., 1992). Space and time dimensions can be disentangled and be assigned to influencing factors. Additionally, the propagation of hydrological signals (e.g. precipitation events) over depth can be assessed (Hohenbrink et al., 2016). This opens up great opportunities for

https://doi.org/10.5194/egusphere-2023-1115
Preprint. Discussion started: 29 June 2023

contributing to the knowledge of soil-hydrological dynamics in agriculture, especially of highly diversified fields that have hardly been studied so far.

We analysed a high-resolution soil moisture data set measured by a novel underground LoRaWAN monitoring system with TDR sensors in different depths of the vadose zone at a spatial-temporally diversified agricultural field in Northeast Germany. The main objective of this study was to identify and quantify the drivers of soil moisture variability within the diversified field by applying PCA. Special focus was put on the spatial and temporal effects of crop diversification and of soil heterogeneities on soil moisture.

2 Materials and methods

2.1 Study site

The study site (52°26'51.8"N 14°08'37.7"E, 66-83 m.a.s.l) is located near the city of Müncheberg in the federal state of Brandenburg in Northeastern Germany. It is located in a hummocky ground moraine landscape that formed during the last glacial periods. Glacial and interglacial processes as well as subsequent erosion resulted in highly heterogeneous soils (Deumlich et al., 2018), being classified as Dystric Podzoluvisols according to the FAO scheme (Fischer et al., 2008). Average total organic carbon content was 0.94% and average total nitrogen content was 0.07% in 0 to 0.3 m soil depth, and average soil pH was 6.12. Between January 1991 and December 2020, the mean annual temperature in Müncheberg was 9.6°C, and the mean annual sum of precipitation was 509 mm (DWD Climate Data Center (CDC), 2021).

2.2 Experimental setup

The data collection was carried out from December 2021 until mid of August 2021 in the patchCROP experiment. It has been set up to study the effect of diversification of cropping schemes on yield, weed, pests and diseases and biodiversity. To that end, single experimental units comprising 30 patches with a size of 0.52 ha (72 m x 72 m) each, following two different yield potential zones with varying soil conditions and site-specific five-year crop rotations (Donat et al., 2022; Grahmann et al., 2021) have been established within a 70 ha large field. For this study, twelve of 30 patches were considered (Table 1). In the cropping season 2020/2021, seven different main crops were grown in these patches. They can be grouped into A) winter crops, B) fallow, followed by summer crops and C) cover crops, followed by summer crops. The remaining area outside of the 30 patches was planted with winter rye. In seven of the twelve considered patches, weed control was carried out with herbicide application, which is in the following entitled as “conventional”. In the remaining five patches, primary weed control was conducted mechanically by harrowing, blind harrowing, and hoeing, and only in the case of high weed pressure, herbicides were applied. This control pattern is in the following entitled as “reduced”.

https://doi.org/10.5194/egusphere-2023-1115
Preprint. Discussion started: 29 June 2023

2.3 Data collection

Soil moisture was recorded by a long-range-wide-area network (LoRaWAN) based monitoring system. In each patch, one LoRaWAN node box (DriBox, Lancashire, UK) was deployed at least 0.3 m below ground to allow normal field traffic and soil tillage. The boxes were installed between August and November 2020. At two georeferenced locations, approximately 2 m from the node boxes TDR-sensors (Acclima TDR310H) were installed in 0.3, 0.6 and 0.9 m depth, respectively, in angles between 45° and 60°.

The data were sent every 20 minutes from the LoRa nodes through a LoRa-WAN Gateway DLOS8 (UP GmbH, Ibbenbüren, Germany) which was equipped with the modem TL-WA7510N (TP Link, Hong Kong) to transfer the data to a cloud from where collected data could be accessed directly after the measurement. The time series included in this study covered the period from December 01, 2020, until August 14, 2021. Figure 1 shows precipitation and temperature at the study site for the study period.

Furthermore, drone imagery from May 31, 2021, was used for vegetation assessment. The drone fixed-wing UAV-based RS eBee platform (SenseFly Ltd., Cheseaux-Lausanne, Switzerland) was operated at noon time and recorded multispectral imagery with a Parrot Sequoia+ camera (green, red, NIR, and red edge bands, spatial resolution of 0.105 m) and thermal imagery of the surface with a senseFly Duet T camera with a spatial resolution of 0.091 m (Table 2). The multispectral imagery was processed with Pix4D to obtain the Normalized Difference Vegetation Index (NDVI), following Eq. (1):

$$NDVI = \frac{NIR-Red}{NIR+Red} \quad (1)$$

in which NIR is the near-infrared and Red the red band of the drone imagery. A digital elevation model with a spatial resolution of 1 m (GeoBasis-DE and LGB, 2021) was used to calculate the slope (ArcGIS 10.7.0; ESRI, 2011) (Table 2).

In October 2019, the soil was scanned with the “Geophilus”- system (Lueck and Ruehlmann, 2013) to map electrical bulk resistivity of the soil as a proxy for soil texture, using reference soil samples to calibrate the readings. Apparent electrical conductivity was measured by pulling one or more sensor pairs mounted on wheels across the field where each pair of sensors measured a different soil depth. Amplitude and phase were measured simultaneously using frequencies from 1 MHz to 1 kHz. Reference soil samples were taken in several points and served as calibration information in order to estimate sand, silt and clay content in the top 0.25 m of soil. A gamma sensor was used to minimize uncertainties but distortion by soil compaction and high water content could not fully be ruled out. The estimated sand content in the upper 0.25 m at the study site varied between 69.1 % and 81.2 % and averaged 79.0 % (Table 1, Figure 2).

2.4 Data processing

Soil moisture data were available at 20-minute intervals. Data gaps due to technical problems or theft of parts of the monitoring system data amounted to 81 out of 257 days of the measuring period. These gaps were not filled. In total, 64 time series could

https://doi.org/10.5194/egusphere-2023-1115
Preprint. Discussion started: 29 June 2023

be used for the analysis, whereas time series of eight sensors were excluded due to frequent malfunctioning. Additional short data gaps for single sensors were interpolated linearly. Ten gaps exceeded the duration of three days with the longest one of 5 days and 3 hours duration. The interpolation was justified as the differences between the values before and after the gaps were within the measuring accuracy of 1 vol-% of the TDR sensors (Acclima Inc., 2019). To ensure equal weighting for the subsequent analysis all soil moisture time series were z-transformed to unit variance and zero mean each (cf. Hohenbrink and Lischeid, 2015).

2.4 Statistical analysis

To identify common temporal patterns among single time series, the soil moisture data set was analysed by a principal component analysis (PCA). In a first step, PCA decomposes the total variance of a multivariate data set into independent fractions called principal components (PCs). The number of PCs is the same as the number of time series in the input data set. Each PC consists of eigenvectors (loadings), scores, and eigenvalues. The scores reflect the temporal dynamics. The importance of single principal components for single sites is represented by the loadings of each PC (Jolliffe, 2002; Lehr and Lischeid, 2020). Loadings are the Pearson correlation coefficients of the single time series of the input data set with the scores of each PC, respectively. The eigenvalues of the single PC are proportional to the variance that they explain. The PCs are sorted in descending order of eigenvalues. Since the input data have been z-transformed, eigenvalues greater than one indicate that the respective PC represents pattern which are relevant for more than one of the observed time series (Kaiser, 1960). More details on principal component analysis for time series analysis are found in Joliffe (2002). The PCA was performed using the *prcomp* function in R (R Development Core Team, 2021). To filter out local effects or the effect of selected PCs from z-transformed observed time series at a specific location, a multiple linear regression was applied between the respective time series and the remaining PCs (Lehr and Lischeid, 2020).

The relations to soil and vegetation parameters were tested by computing the Pearson correlation coefficients between the scores and arithmetic mean values of all input time series as well as the Pearson correlation coefficients between loadings and sand content, sensor depth, antecedent z-transformed water contents, slope, and the drone imagery products from May 31, 2021 (NDVI and surface temperature). Eventually, the Wilcoxon-Mann-Whitney test was applied to check whether loadings can be grouped by management parameters (crops, cover crops, weeding management).

All statistical analyses were conducted with R (R Development Core Team, 2021).

3 Results

The principal component analysis yielded five components with Eigenvalues exceeding one. They accounted for more than 97% of the variance of the total data set (Table 4).

https://doi.org/10.5194/egusphere-2023-1115
Preprint. Discussion started: 29 June 2023

3.1 First principal component

The first principal component explained 72.3% of the data set's spatial and temporal variance. All loadings on the first PC were negative. The Pearson correlation coefficient of the scores of the first principal component with the mean values of all input time series was less than - 0.999 ($p < 0.01$). Thus the time series of the scores of this component with reversed sign represented the mean behaviour of soil moisture driven by external factors such as precipitation, temperature, and seasons in general which affected all time series in the same way, although to different degrees (cf., Hohenbrink et al., 2016; Lischeid et al., 2021).

3.2 Second principal component

The second principal component explained 17.0% of the total variance. The loadings ranged from -0.801 to 0.760 with a median of -0.030 (Figure 3). The loadings showed a crop type specific pattern. All winter crops (barley, oats, rye) had positive loadings with only one exception in 0.9 m depth. The summer crops maize, soy, and sunflower exhibited negative loadings. In contrast, the summer crop lupine exhibited mostly positive loadings, similar to the winter crops, although of slightly smaller magnitude. According to the Wilcoxon-Mann test the group of barley, oats, rye, and lupine differed significantly from the group of maize, soy, and sunflower.

The scores of the principal components constitute time series. Every observed time series can be presented at arbitrary precision as a combination of various principal components. Moreover, generating synthetic time series as linear combinations of the first and the second principal components helps to assign the second principal component to a specific effect. To that end scores of that component have either been added to or subtracted from those of the first component using arbitrarily selected factors (Figure 4). A positive factor would be typical for winter crops (blue line) which load positively on that component. The opposite holds for the summer crops (orange line). Both lines plot very close to each other in February and March. In contrast, the orange line is underneath the blue line in December and January, indicating lower soil moisture at the summer crop patches. The inverse holds for the subsequent summer period starting in early June, pointing to earlier and more rapid water uptake of the winter crops.

Lupine and sunflower were the summer crops which were sown first (March 30, 2021, and April 2, 2021, respectively). Maize was sown on April 16, 2021, and soy on May 15, 2021. The loadings of lupine which were rather performing like winter crops than summer crops indicated that lupine showed an early onset of intensive evapotranspiration, compared to other summer crops, especially sunflower which was sown at the same time.

For further investigation of the vegetation effect in PCs, the loadings of PC2 were compared to drone imagery taken on May 31, 2021, when all patches were covered by crops. The second PC's loadings of the time series from different sensors were compared to the Normalized Difference Vegetation Index (NDVI) and surface temperature of the respective sensor location as a proxy for actual evapotranspiration. As shown in Table 3, the NDVI was positively correlated with the loadings while

https://doi.org/10.5194/egusphere-2023-1115
Preprint. Discussion started: 29 June 2023

surface temperature exhibited negative correlations, indicating higher evapotranspiration. This holds for sensors from all depths but was the closest for 0.9 m depth (Pearson correlation of r = -0.916 for surface temperature and of r = 0.940 for NDVI).

3.3 Third principal component

The third PC explained 4.1% of the total data set's variance. Loadings ranged between -0.787 and 0.244 with a median of 0.006. Extreme loadings (<-0.25) were found only for sensors in 0.9 m depth in patches 66, 89, 95 and 102 (Figure 5). These patches are located along a line that roughly follows a west-to-east direction (Figure 2). Loadings were closely related to the minima of the z-transformed soil moisture in the period from December to February (r = 0.70). Strong negative loadings on the third principal component imply delayed response to rainstorms and reduced subsequent dehydration (Figure 6).

3.4 Fourth principal component

The fourth PC explained 2.2% of the total data set's variance. The loadings were clustered by treatment groups. All fallow patches showed consistent positive loadings while the patches which were covered by winter crops (treatment group A) showed mainly negative loadings except in patch 95 where the loadings of the two sensors in 0.3 m depth were slightly above zero (Figure 7). According to the Wilcoxon-Mann test treatment group B differed significantly from group A and C whereas there was no significant difference between group A and C. In contrast to treatment groups A and B, patches that were covered by the cover crop phacelia during the winter months, did not show one-directional loadings.

Besides showing a treatment group pattern, the loadings of PC4 also correlated with the sand content in a 1 m radius around the sensor locations in the upper 0.25 m (r = 0.67). Due to a lack of sand content data for deeper layers, only data from the sensor depth of 0.3 m were analysed. The second-best correlation coefficient is found for PC3 with -0.36.

Figure 8 illustrates the effect of the fourth PC on time series. A positive factor would be typical for more sandy soils and for patches with fallow in autumn and winter (blue line). In contrast the orange line depicts behaviour in more loamy soils and for winter crops. The latter line exhibits slightly more delayed responses to rainstorms and subsequent less steep recovery. This pattern would be consistent with a lower sand content.

3.5 Fifth principal component

The fifth PC explained 1.67 % of the data set's variance. The loadings showed a depth-related pattern. All time series from 0.3 m exhibited negative loadings with two minor exceptions whereas all time series from 0.9 m depth showed positive loadings throughout, and time series from 0.6 m depth plot in between. Loadings in 0.6 m depth and 0.9 m depth were mostly more similar to each other than to the loadings of 0.3 m depth (Figure 9). The Pearson correlation coefficient between loadings and depth was r = 0.710 ($p < 0.05$). Thus it can be concluded that the fifth PC reflected the effect of soil depth. Note that this effect differed between crops. The three most negative loadings were found in maize patches while the three most positive loadings were found in sunflower patches.

https://doi.org/10.5194/egusphere-2023-1115
Preprint. Discussion started: 29 June 2023

The hydrological signal after rainfall events exhibits damping over depth (blue line) while sensors in the upper layer react with a higher sensitivity (orange line) to weather conditions (Figure 10).

4 Discussion

The first five principal components described about 97% of the variance of the data set, which consisted of observed time series from 64 soil moisture probes. That results pointed to considerable redundancies between the effects of soil heterogeneities and of twelve different crops and management schemes (Table 1). Thereof the first principal component captured 72% of the total variance. Consequently, 72% of the observed dynamics could be described by a lumped model that would not consider any within-field heterogeneity. This figure is in the range of similar studies. In the study of Martini et al. (2017) the first PC explained 58% of the variance of a data set that comprised both agricultural fields as well as grassland transects. Lischeid et al. (2017) ascribed 70% of the variance of a forest soil hydrological data set to a single component. In the study by Hohenbrink et al. (2016) 85% of the variance of soil hydrological data in a set of arable field experiments with two different crop rotation schemes was assigned to a common dynamic.

4.1 Crop effects

As Korres et al. (2015) stated, the main causes for spatial variability of soil moisture in agricultural fields besides soil parameters are vegetation and management (e.g. planting and harvesting dates). The quantification of these effects is highly important, for instance for hydrological applications and adopted management practices in agriculture (Hupet and Vanclooster, 2002). Joshi and Mohanty (2010) investigated the spatial soil moisture variability on the field to regional scale in the Southern Great Plains regions in the US by means of PCA and assessed the effect of vegetation as limited since none of the first seven PC showed strong correlations with vegetation parameters. In Western China, Wang et al. (2019) used a non-linear Granger causality framework and quantified the vegetation effect on soil moisture variability with up to 8.2%.

In this study, conducted at the field scale, around 17% of the total variance was attributed to the vegetation effect. When not considering the temporal component reflected by PC1 and thus only looking at the spatial variability, 61% of the variance is caused by the vegetation effect reflected by PC2. Korres et al. (2010) also used PCA to quantify spatial variabilities of soil moisture within a cropped area but did not find such a pronounced vegetation effect. In their study more than two thirds of the spatial variability was related to soil parameters and topography. In contrast, the strong influence of vegetation in our study may be due to the high level of crop diversification. Within single crop fields vegetation effects are observable due to heterogeneous biomass or root development (Brown et al., 2021; Korres et al., 2010), but may be of a lower magnitude compared to fragmented field arrangements with different crops. The high impact of the crop diversification on soil moisture variability is also visible when comparing our results to the results of a field under comparable conditions in the same region with only two crop rotations in which only 3.8 % was explained by different crop rotations (Hohenbrink et al., 2016). Yang et al. (2015) remarked that the differences in soil moisture between vegetation types with different biomass is profound especially

https://doi.org/10.5194/egusphere-2023-1115
Preprint. Discussion started: 29 June 2023

in deeper layers. In this study, however, the decreasing gradient of the explained variance over depth was indicating the opposite. In the first layer, the effect of vegetation caused the highest variance in soil moisture.

It needs to be considered that the proportion of the vegetation effect on soil moisture variability does not only vary spatially and over depth, but also over time. Under dry conditions, soil-plant interactions prevail while under moist conditions, percolation behaviour is predominant (Baroni et al., 2013). In our study, the variability of the vegetation effect over time is observable in the temporal development of the scores. In accordance with literature, the absolute values of the scores of PC2, representing differences between the contrasting seasonality of crops, are highest in the dry months May to August. In the moist winter months January to March, as well as during the heavy rainfall event in July, the scores of PC2 are relatively small, showing that spatial variability at that time is caused by other factors.

The second principal component clearly differentiated between winter and summer crops which was driven by the different seasonal patterns of root water uptake (Figure 3). In contrast, the fourth component separated winter crops and fallow (Figure 7). Note that the term “fallow” refers to crop cover in autumn and winter only. Phacelia is grown as a cover crop and usually dies off in frost periods. However, due to rather mild winter temperature this did only partly happen in the study period. Thus some Phacelia patches exhibited negative loadings, similarly to the winter crop patches. Hence the fourth component obviously reflected the effect of plant cover in the winter period which can hardly be ascribed to different patterns of root water uptake. According to this component, soil moisture at the fallow patches resembled more that of sandy soils, and that of winter crop patches more that of loamy soils. That feature could point to a soil carbon effect on the soil’s water holding capacity: Only at the winter crop sites organic carbon in soil increased continuously due to root growth and root exudation, whereas mineralisation reduced the organic carbon stock at the fallow sites. Effects of dense living root networks on soil hydraulic conductivity have been reported, e.g., by Scholl et al., (2014), Zhang et al. (2021) and Lange et al. (2013). Further soil-vegetation interactions might play a role, such as soil organic matter from cover crops and plant residues (Manns et al., 2014; Rossini et al., 2021). Although this effect constituted only a minor share of soil moisture variance (Table 4), it was clearly discernible as a separate principal component. This effect would be worth to be tested in more detailed studies. If it were to be confirmed, it would be a good example for how plants shape their environment.

4.2 Soil texture effects

Texture is another highly important spatial variable that affects soil moisture. The pore size distribution which is directly linked to texture has great influence on wetting processes as well as on the water retention capacity of soil (Krauss et al., 2010; Rossini et al., 2021). Furthermore, texture influences the evapotranspiration which is another main factor controlling soil moisture (Pan and Peters-Lidard, 2008). For coarse grained soils as they are present in this case study, the water retention capacity is small, resulting in enhanced seepage fluxes (Scheffer and Schachtschabel, 2002; Krauss et al. 2010).

Loadings on the third principal component were not related to crop types. In contrast, a spatial pattern emerged: Only sensors from 0.9 m depth from six adjacent patches exhibited strongly negative loadings (Figure 2) whereas all other sensors showed minor positive or negative loadings. This points to an effect of subsoil substrates, that is higher loam content and consequently

https://doi.org/10.5194/egusphere-2023-1115
Preprint. Discussion started: 29 June 2023

higher water holding capacity. That would be consistent with delayed response to seepage fluxes and reduced desiccation in the vegetation period (Figure 6).

Whereas the third principal component seems to reflect a local peculiarity, the fifth component obviously grasps a more generic feature. Loadings on this component are clearly related with depth (Figure 6). Strong positive loadings indicate a strongly damped behaviour of soil moisture time series (Figure 10). Hohenbrink and Lischeid (2015) combined a hydrological model and principal component analysis to study the effect of soil depth and soil texture on damping of the input signal in more detail. A subsequent field study proved the relevance of that effect in a real world setting (Hohenbrink et al., 2016). Moreover, Thomas et al. (2012) found that damping accounted for a large share of variance in a set of hydrographs from a region of 30,000 km^2. Damping was also the most relevant driver of spatial variance in a set of time series of groundwater head at about the same scale (Lischeid et al., 2021).

5 Conclusion

To disentangle and to quantify different effects of environmental processes in complex settings is a key challenge of agricultural and environmental research. It is an indispensable prerequisite for tailored field and crop management. Mechanistic models are a way to upscale findings from numerous single cause-single effect studies. But there is urgent need to further validate model results and to study interactions between various effects in a systematic way. This study focuses on the interplay between crops and soil heterogeneities in terms of soil moisture dynamics based on a comprehensive real-world data set. More than 97% of the observed spatial and temporal variance was assigned to five different effects. Meteorological drivers explained 72.3% of the total variance. Different seasonal patterns of root water uptake of winter crops compared to summer crops accounted for another 17.0% of variance. An additional share of 2.2% of variance seemed to be related to the effects of a living rooting system on soil hydraulic properties. Heterogeneity of subsoil substrates explained 4.1 % of variance, and the damping effect of input signals in the soil another 1.7%. To summarize, plant-related direct and indirect effects accounted for 19.2% of the variance, and soil-related effects only for 5.8%. In particular, the plant-induced effects on soil hydraulic properties would be worthwhile to be studied in more detail. Adequate crop selection could be a management option to encounter the increasing drought risk in the study region.

This information will contribute to elucidate management effects as well as to develop both parsimonious and tailored mechanistic models. In this regard, principal component analysis of soil moisture time series performed as a powerful diagnostic tool and is highly recommended.

https://doi.org/10.5194/egusphere-2023-1115
Preprint. Discussion started: 29 June 2023

Acknowledgments

The maintenance of the patchCROP experimental infrastructure and the LoRaWAN soil sensor system is ensured by the Leibniz Centre for Agricultural Landscape Research. The authors acknowledge the additional support from the German Research Foundation under Germany's Excellence Strategy, EXC-2070 – 390732324 – PhenoRob for patchCROP related research activities.

The authors thank Gerhard Kast, Thomas von Oepen, Lars Richter, Robert Zieciak, Sigrid Ehlert and Motaz Abdelaziz for their dedicated support in maintenance of the monitoring system and data collection.

Competing interests

The authors declare that they have no conflict of interest.

References

Acclima Inc.: True TDR310H. Soil-Water-Temperature-BEC-Sensor, 2019.

Alhameid, A., Singh, J., Sekaran, U., Ozlu, E., Kumar, S., and Singh, S.: Crop rotational diversity impacts soil physical and hydrological properties under long-term no- and conventional-till soils, Soil Res., 58, 84, https://doi.org/10.1071/SR18192, 2020.

Baroni, G., Ortuani, B., Facchi, A., and Gandolfi, C.: The role of vegetation and soil properties on the spatio-temporal variability of the surface soil moisture in a maize-cropped field, Journal of Hydrology, 489, 148–159, https://doi.org/10.1016/j.jhydrol.2013.03.007, 2013.

Birthal, P. S. and Hazrana, J.: Crop diversification and resilience of agriculture to climatic shocks: Evidence from India, Agricultural Systems, 173, 345–354, https://doi.org/10.1016/j.agsy.2019.03.005, 2019.

Bretherton, C. S., Smith, C., and Wallace, J. M.: An intercomparison of methods for finding coupled patterns in climate data, Journal of Climatology, 5, 541–560, 1992.

Brocca, L., Melone, F., Moramarco, T., and Morbidelli, R.: Spatial-temporal variability of soil moisture and its estimation across scales, Water Resour. Res., 46, https://doi.org/10.1029/2009WR008016, 2010.

Brown, M., Heinse, R., Johnson-Maynard, J., and Huggins, D.: Time-lapse mapping of crop and tillage interactions with soil water using electromagnetic induction, Vadose zone j., 20, https://doi.org/10.1002/vzj2.20097, 2021.

Cardell-Oliver, R., Hübner, C., Leopold, M., and Beringer, J.: Dataset: LoRa Underground Farm Sensor Network, in: Proceedings of the 2nd Workshop on Data Acquisition To Analysis - DATA'19, the 2nd Workshop, New York, NY, USA, 26–28, https://doi.org/10.1145/3359427.3361912, 2019.

Deumlich, D., Ellerbrock, R. H., and Frielinghaus, Mo.: Estimating carbon stocks in young moraine soils affected by erosion, CATENA, 162, 51–60, https://doi.org/10.1016/j.catena.2017.11.016, 2018.

https://doi.org/10.5194/egusphere-2023-1115
Preprint. Discussion started: 29 June 2023

Donat, M., Geistert, J., Grahmann, K., Bloch, R., and Bellingrath-Kimura, S. D.: Patch cropping- a new methodological approach to determine new field arrangements that increase the multifunctionality of agricultural landscapes, Computers and Electronics in Agriculture, 197, 106894, https://doi.org/10.1016/j.compag.2022.106894, 2022.

DWD Climate Data Center (CDC): Historische tägliche Stationsbeobachtungen (Temperatur, Druck, Niederschlag, Sonnenscheindauer, etc.) für Deutschland, Version v21.3, 2021.

Fischer, G. F., Nachtergaele, S., Prieler, S., van Velthuizen, H. T., Verelst, L., and Wisberg, D.: Global Agro-ecological Zones Assessment for Agriculture (GAEZ 2008), IIASA, Laxenburg, Austria and FAO, Rome, Italy, 2008.

GeoBasis-DE and Landesvermessung und Geobasisinformation Brandenburg (LGB): Digitales Geländemodell (DGM), Landesvermessung und Geobasisinformation Brandenburg (LGB), Potsdam, Germany, 2021.

Grahmann, K., Reckling, M., Hernandez-Ochoa, I., and Ewert, F.: An agricultural diversification trial by patchy field arrangements at the landscape level: The landscape living lab "patchCROP," in: Aspects of Applied Biology, Intercropping for sustainability: Research developments and their application, 385–391, 2021.

Hohenbrink, T. L. and Lischeid, G.: Does textural heterogeneity matter? Quantifying transformation of hydrological signals in soils, Journal of Hydrology, 523, 725–738, https://doi.org/10.1016/j.jhydrol.2015.02.009, 2015.

Hohenbrink, T. L., Lischeid, G., Schindler, U., and Hufnagel, J.: Disentangling the Effects of Land Management and Soil Heterogeneity on Soil Moisture Dynamics, Vadose Zone Journal, 15, https://doi.org/10.2136/vzj2015.07.0107, 2016.

Hupet, F. and Vanclooster, M.: Intraseasonal dynamics of soil moisture variability within a small agricultural maize cropped field, Journal of Hydrology, 261, 86–101, 2002.

Jolliffe, I. T.: Principal component analysis. Springer Series in Statistics, Springer, New York, 2002.

Joshi, C. and Mohanty, B. P.: Physical controls of near-surface soil moisture across varying spatial scales in an agricultural landscape during SMEX02: Physical controls of soil moisture, Water Resour. Res., 46, https://doi.org/10.1029/2010WR009152, 2010.

Kaiser, H. F.: The Application of Electronic Computers to Factor Analysis, Educ.Psychol. Measur., 20, https://doi.org/10.1177/001316446002000116, 1960.

Karlen, D. L., Hurley, E. G., Andrews, S. S., Cambardella, C. A., Meek, D. W., Duffy, M. D., and Mallarino, A. P.: Crop Rotation Effects on Soil Quality at Three Northern Corn/Soybean Belt Locations, Agron.j., 98, 484–495, https://doi.org/10.2134/agronj2005.0098, 2006.

Khan, H., Farooque, A. A., Acharya, B., Abbas, F., Esau, T. J., and Zaman, Q. U.: Delineation of Management Zones for Site-Specific Information about Soil Fertility Characteristics through Proximal Sensing of Potato Fields, Agronomy, 10, 1854, https://doi.org/10.3390/agronomy10121854, 2020.

Korres, W., Koyama, C. N., Fiener, P., and Schneider, K.: Analysis of surface soil moisture patterns in agricultural landscapes using Empirical Orthogonal Functions, Hydrol. Earth Syst. Sci., 14, 751–764, https://doi.org/10.5194/hess-14-751-2010, 2010.

Korres, W., Reichenau, T. G., Fiener, P., Koyama, C. N., Bogena, H. R., Cornelissen, T., Baatz, R., Herbst, M., Diekkrüger, B., Vereecken, H., and Schneider, K.: Spatio-temporal soil moisture patterns – A meta-analysis using plot to catchment scale data, Journal of Hydrology, 520, 326–341, https://doi.org/10.1016/j.jhydrol.2014.11.042, 2015.

https://doi.org/10.5194/egusphere-2023-1115
Preprint. Discussion started: 29 June 2023

Krauss, L., Hauck, C., and Kottmeier, C.: Spatio-temporal soil moisture variability in Southwest Germany observed with a new monitoring network within the COPS domain, metz, 19, 523–537, https://doi.org/10.1127/0941-2948/2010/0486, 2010.

Lange, B., Germann, P. F., and Lüscher, P.: Greater abundance of Fagus sylvatica in coniferous flood protection forests due to climate change: impact of modified root densities on infiltration, Eur J Forest Res, 132, 151–163, https://doi.org/10.1007/s10342-012-0664-z, 2013.

Lehr, C. and Lischeid, G.: Efficient screening of groundwater head monitoring data for anthropogenic effects and measurement errors, Hydrol. Earth Syst. Sci., 24, 501–513, https://doi.org/10.5194/hess-24-501-2020, 2020.

Lischeid, G., Frei, S., Huwe, B., Bogner, C., Lüers, J., Babel, W., and Foken, T.: Catchment Evapotranspiration and Runoff, in: Energy and Matter Fluxes of a Spruce Forest Ecosystem, vol. 229, Springer, Cham, Cham, 355–375, 2017.

Lischeid, G., Dannowski, R., Kaiser, K., Nützmann, G., Steidl, J., and Stüve, P.: Inconsistent hydrological trends do not necessarily imply spatially heterogeneous drivers, Journal of Hydrology, 596, 126096, https://doi.org/10.1016/j.jhydrol.2021.126096, 2021.

Lloret, J., Sendra, S., Garcia, L., and Jimenez, J. M.: A Wireless Sensor Network Deployment for Soil Moisture Monitoring in Precision Agriculture, Sensors, 21, 7243, https://doi.org/10.3390/s21217243, 2021.

Lueck, E. and Ruehlmann, J.: Resistivity mapping with Geophilus Electricus - Information about lateral and vertical soil heterogeneity, Geoderma, 199, 2–11, https://doi.org/10.1016/j.geoderma.2012.11.009, 2013.

Mahmood, R., Littell, A., Hubbard, K. G., and You, J.: Observed data-based assessment of relationships among soil moisture at various depths, precipitation, and temperature, Applied Geography, 34, 255–264, https://doi.org/10.1016/j.apgeog.2011.11.009, 2012.

Martini, E., Wollschläger, U., Musolff, A., Werban, U., and Zacharias, S.: Principal Component Analysis of the Spatiotemporal Pattern of Soil Moisture and Apparent Electrical Conductivity, Vadose Zone Journal, 16, vzj2016.12.0129, https://doi.org/10.2136/vzj2016.12.0129, 2017.

Nied, M., Hundecha, Y., and Merz, B.: Flood-initiating catchment conditions: a spatio-temporal analysis of large-scale soil moisture patterns in the Elbe River basin, Hydrol. Earth Syst. Sci., 17, 1401–1414, https://doi.org/10.5194/hess-17-1401-2013, 2013.

Pan, F. and Peters-Lidard, C. D.: On the Relationship Between Mean and Variance of Soil Moisture Fields, JAWRA Journal of the American Water Resources Association, 44, 235–242, https://doi.org/10.1111/j.1752-1688.2007.00150.x, 2008.

Paroda, Raj. S., Suleimenov, M., Yusupov, H., Kireyev, A., Medeubayev, R., Martynova, L., and Yusupov, K.: Crop Diversification for Dryland Agriculture in Central Asia, in: CSSA Special Publications, edited by: Rao, S. C. and Ryan, J., Crop Science Society of America and American Society of Agronomy, Madison, WI, USA, 139–150, https://doi.org/10.2135/cssaspecpub32.c9, 2015.

Placidi, P., Morbidelli, R., Fortunati, D., Papini, N., Gobbi, F., and Scorzoni, A.: Monitoring Soil and Ambient Parameters in the IoT Precision Agriculture Scenario: An Original Modeling Approach Dedicated to Low-Cost Soil Water Content Sensors, Sensors, 21, 5110, https://doi.org/10.3390/s21155110, 2021.

Prakosa, S. W., Faisal, M., Adhitya, Y., Leu, J.-S., Köppen, M., and Avian, C.: Design and Implementation of LoRa Based IoT Scheme for Indonesian Rural Area, Electronics, 10, 77, https://doi.org/10.3390/electronics10010077, 2021.

https://doi.org/10.5194/egusphere-2023-1115
Preprint. Discussion started: 29 June 2023

R Development Core Team: R: A Language and Environment for Statistical Computing, R Foundation for Statistical Computing (Version 4.1.0, http://www.R-project.org), Vienna, Austria, 2021.

Rodriguez, C., Mårtensson, L.-M. D., Jensen, E. S., and Carlsson, G.: Combining crop diversification practices can benefit cereal production in temperate climates, Agron. Sustain. Dev., 41, 48, https://doi.org/10.1007/s13593-021-00703-1, 2021.

Rossini, P. R., Ciampitti, I. A., Hefley, T., and Patrignani, A.: A soil moisture-based framework for guiding the number and location of soil moisture sensors in agricultural fields, Vadose zone j., 20, https://doi.org/10.1002/vzj2.20159, 2021.

Salam, A.: Internet of Things for Sustainable Community Development: Wireless Communications, Sensing, and Systems, Springer International Publishing, Cham, Switzerland, https://doi.org/10.1007/978-3-030-35291-2, 2020.

Salam, A. and Raza, U.: Signals in the Soil: Developments in Internet of Underground Things, Springer International Publishing, Cham, Switzerland, https://doi.org/10.1007/978-3-030-50861-6, 2020.

Scheffer, F. and Schachtschabel, P.: Lehrbuch der Bodenkunde, 15th ed., Spektrum Akademischer Verlag GmbH. Berlin, Heidelberg, https://doi.org/10.1007/978-3-662-55871-3, 2002.

Scholl, P., Leitner, D., Kammerer, G., Loiskandl, W., Kaul, H.-P., and Bodner, G.: Root induced changes of effective 1D hydraulic properties in a soil column, Plant Soil, 381, 193–213, https://doi.org/10.1007/s11104-014-2121-x, 2014.

Si, B. C.: Spatial Scaling Analyses of Soil Physical Properties: A Review of Spectral and Wavelet Methods, Vadose Zone Journal, 7, 547–562, https://doi.org/10.2136/vzj2007.0040, 2008.

Strebelle, S., Payrazyan, K., and Caers, J.: Modeling of a Deepwater Turbidite Reservoir Conditional to Seismic Data Using Principal Component Analysis and Multiple-Point Geostatistics, SPE Journal, 8, 227–235, https://doi.org/10.2118/85962-PA, 2003.

Tamburini, G., Bommarco, R., Wanger, T. C., Kremen, C., van der Heijden, M. G. A., Liebman, M., and Hallin, S.: Agricultural diversification promotes multiple ecosystem services without compromising yield, Sci. Adv., 6, eaba1715, https://doi.org/10.1126/sciadv.aba1715, 2020.

Taylor, J. and Whelan, B.: A General Introduction to Precision Agriculture, 2010.

Thomas, B., Lischeid, G., Steidl, J., and Dannowski, R.: Regional catchment classification with respect to low flow risk in a Pleistocene landscape, Journal of Hydrology, 475, 392–402, https://doi.org/10.1016/j.jhydrol.2012.10.020, 2012.

Trnka, M., Rötter, R. P., Ruiz-Ramos, M., Kersebaum, K. C., Olesen, J. E., Žalud, Z., and Semenov, M. A.: Adverse weather conditions for European wheat production will become more frequent with climate change, Nature Clim Change, 4, 637–643, https://doi.org/10.1038/nclimate2242, 2014.

Vereecken, H., Huisman, J. A., Pachepsky, Y., Montzka, C., van der Kruk, J., Bogena, H., Weihermüller, L., Herbst, M., Martinez, G., and Vanderborght, J.: On the spatio-temporal dynamics of soil moisture at the field scale, Journal of Hydrology, 516, 76–96, https://doi.org/10.1016/j.jhydrol.2013.11.061, 2014.

Wang, Y., Yang, J., Chen, Y., Fang, G., Duan, W., Li, Y., and De Maeyer, P.: Quantifying the Effects of Climate and Vegetation on Soil Moisture in an Arid Area, China, Water, 11, 767, https://doi.org/10.3390/w11040767, 2019.

Yang, L., Chen, L., and Wei, W.: Effects of vegetation restoration on the spatial distribution of soil moisture at the hillslope scale in semi-arid regions, CATENA, 124, 138–146, https://doi.org/10.1016/j.catena.2014.09.014, 2015.

https://doi.org/10.5194/egusphere-2023-1115
Preprint. Discussion started: 29 June 2023

Zhang, J., Li, Y., Yang, T., Liu, D., Liu, X., and Jiang, N.: Spatiotemporal variation of moisture in rooted-soil, CATENA, 200, 105144, https://doi.org/10.1016/j.catena.2021.105144, 2021.

Zhao, Y., Peth, S., Wang, X. Y., Lin, H., and Horn, R.: Controls of surface soil moisture spatial patterns and their temporal stability in a semi-arid steppe, Hydrol. Process., 24, 2507–2519, https://doi.org/10.1002/hyp.7665, 2010.

Figures and Tables

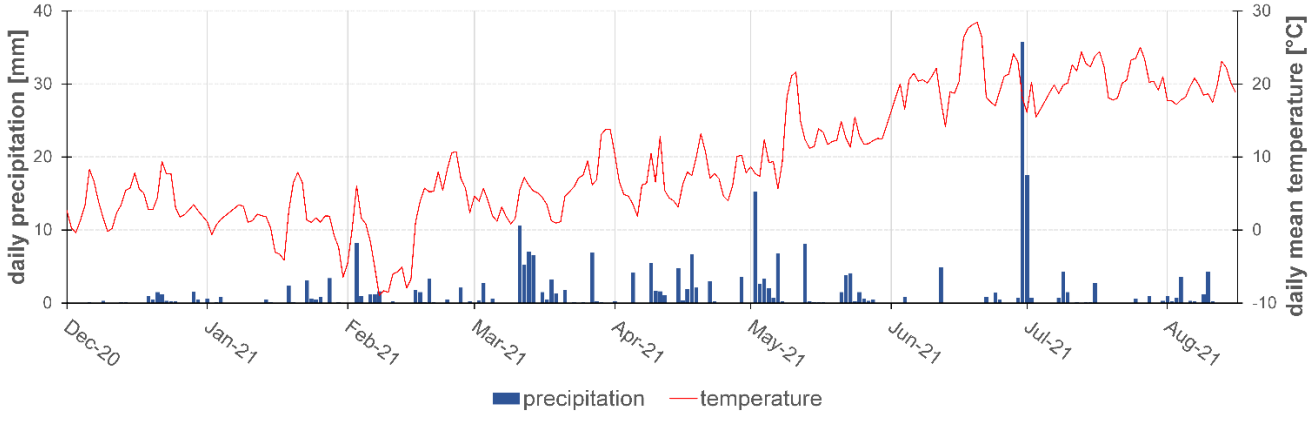

Figure 1: Daily precipitation and daily mean temperature from 2020-12-01 until 2021-08-15 measured at the field experiment.

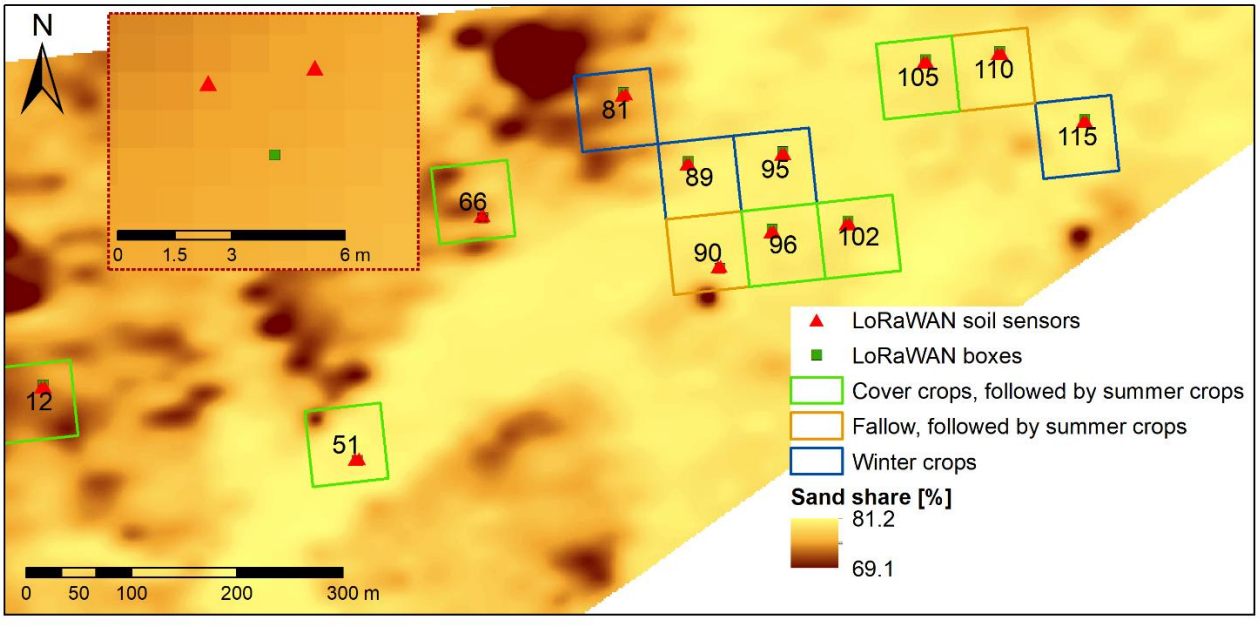

Figure 2: Sand content down to 0.25 m depth and location of the analysed patches including soil sensors under different crop rotations in the landscape laboratory patchCROP. The inset shows sensor and box location within one of the patches.

https://doi.org/10.5194/egusphere-2023-1115
Preprint. Discussion started: 29 June 2023

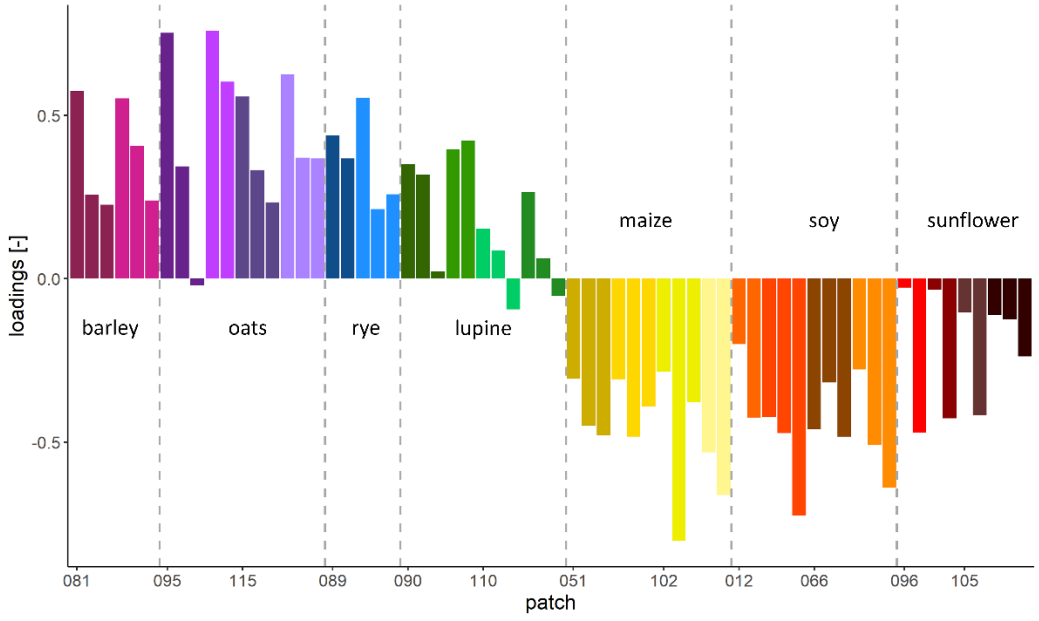

Figure 3: Loadings of time series on the second principal component. Bars represent individual time series grouped by patch ID and sorted and coloured by crop. Bars of the same colour are sorted by sensor depth, increasing from left to right (0.3 m, 0.6 m, 0.9 m).

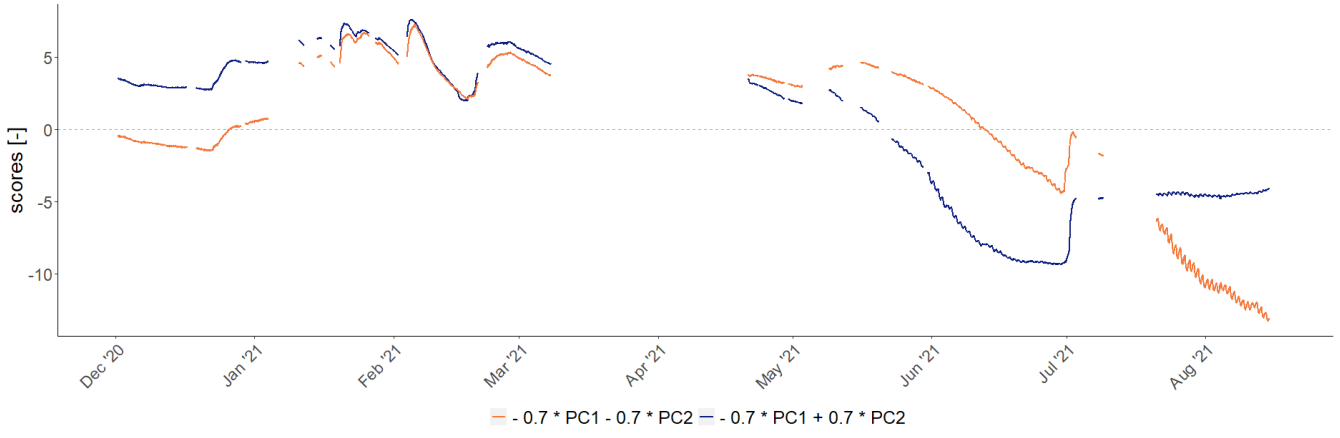

Figure 4: Effect of the second principal component on modification of the general mean behaviour which is presented by the first principal component.

https://doi.org/10.5194/egusphere-2023-1115
Preprint. Discussion started: 29 June 2023

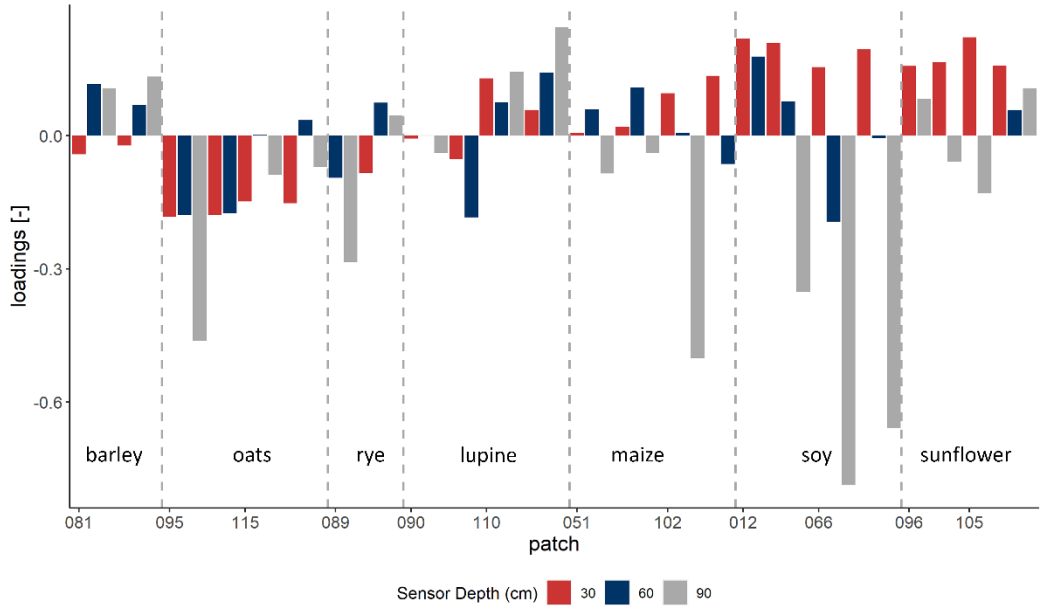

Figure 5: Loadings of time series on the third principal component. Bars represent individual time series grouped by patch ID, sorted by crop.

470

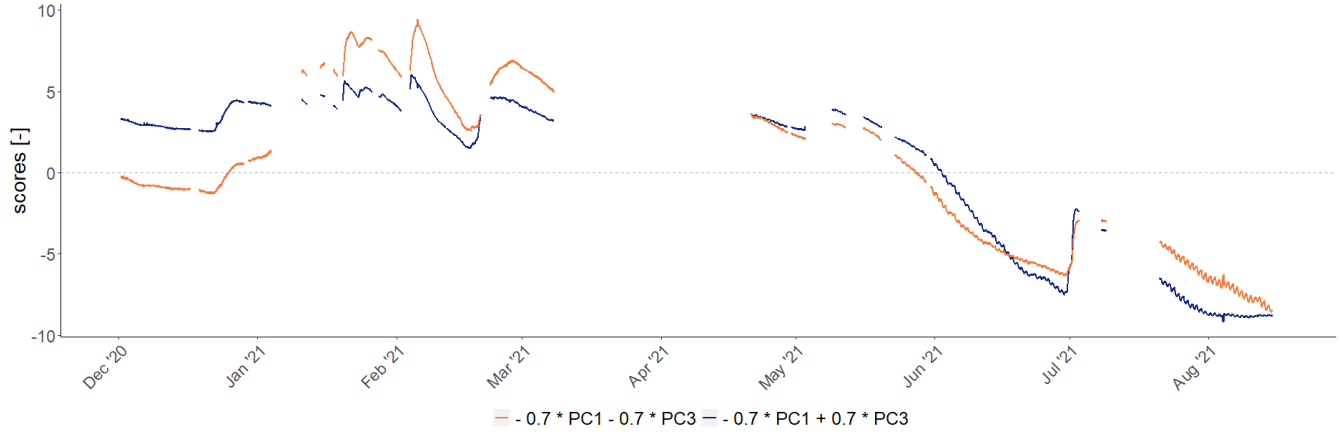

Figure 6: Effect of the third principal component on modification of the general mean behaviour which is presented by the first principal component.

https://doi.org/10.5194/egusphere-2023-1115
Preprint. Discussion started: 29 June 2023

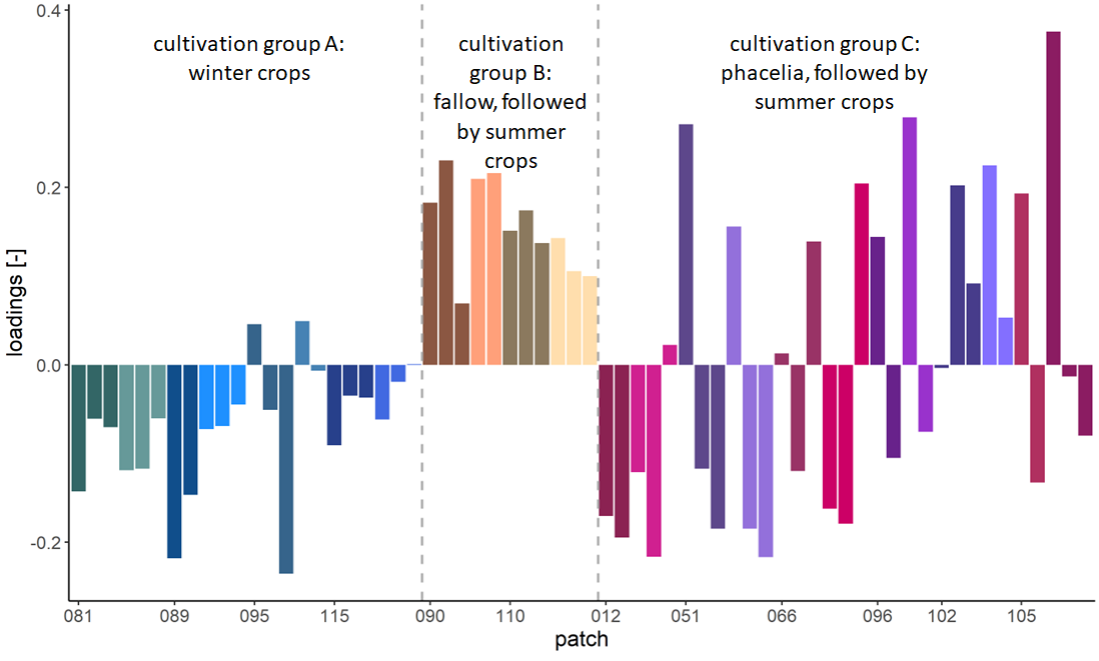

475 **Figure 7: Loadings of time series on the fourth principal component. Bars represent individual time series grouped by patch ID, sorted and coloured by treatment group. Bars of the same colour are sorted by sensor depth, increasing from left to right.**

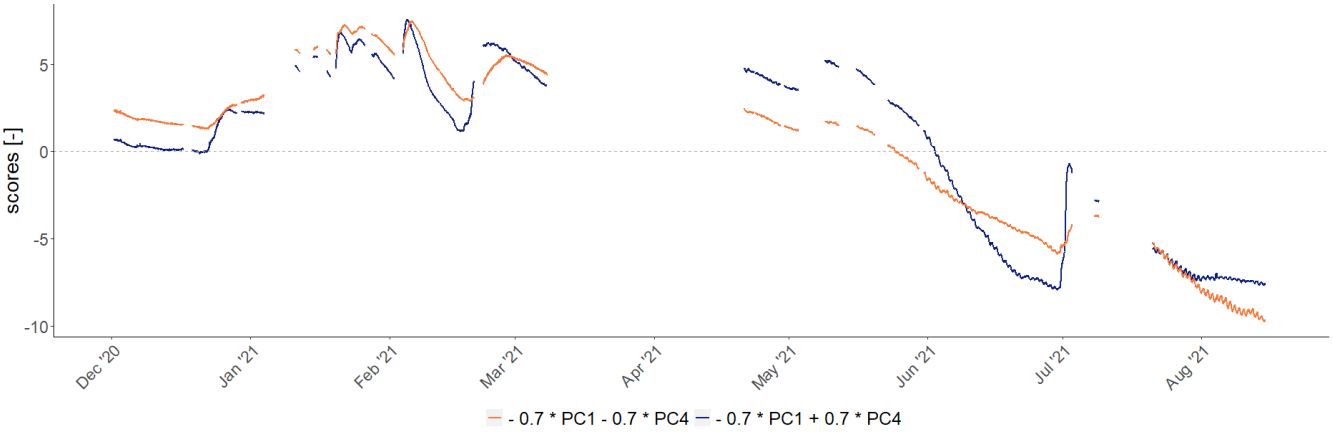

Figure 8: Effect of the fourth principal component on modification of the general mean behaviour which is presented by the first principal component.

480

https://doi.org/10.5194/egusphere-2023-1115
Preprint. Discussion started: 29 June 2023

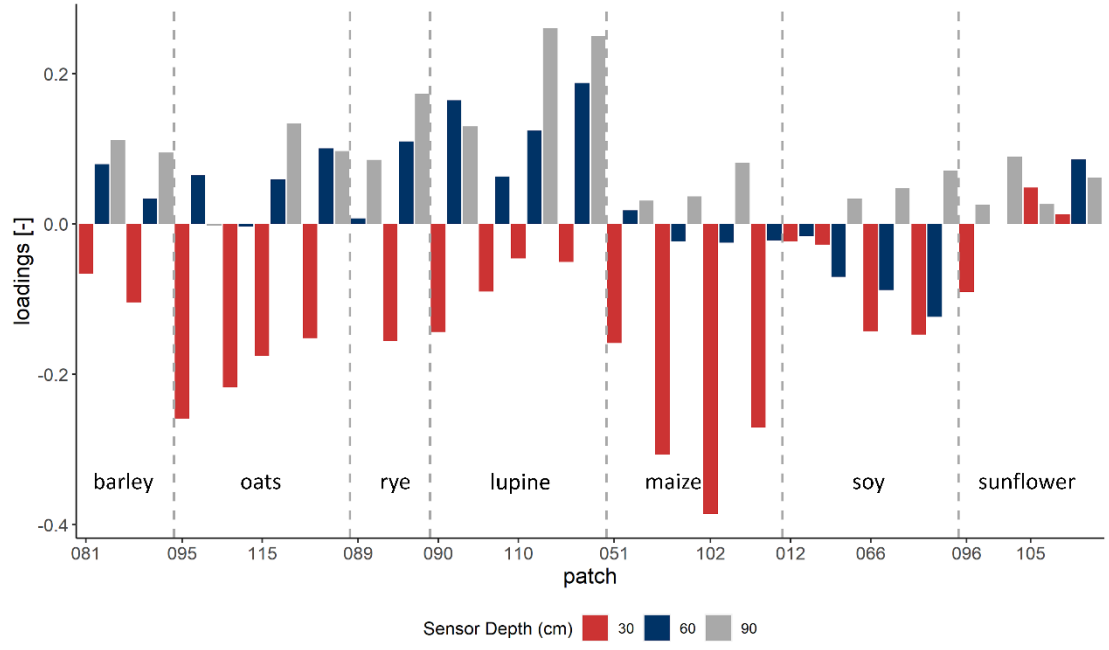

Figure 9: Loadings of time series on the fifth principal component. Bars represent individual time series grouped by patch ID, sorted by crop. Within each patch, time series are sorted by sensor depth, increasing from left to right.

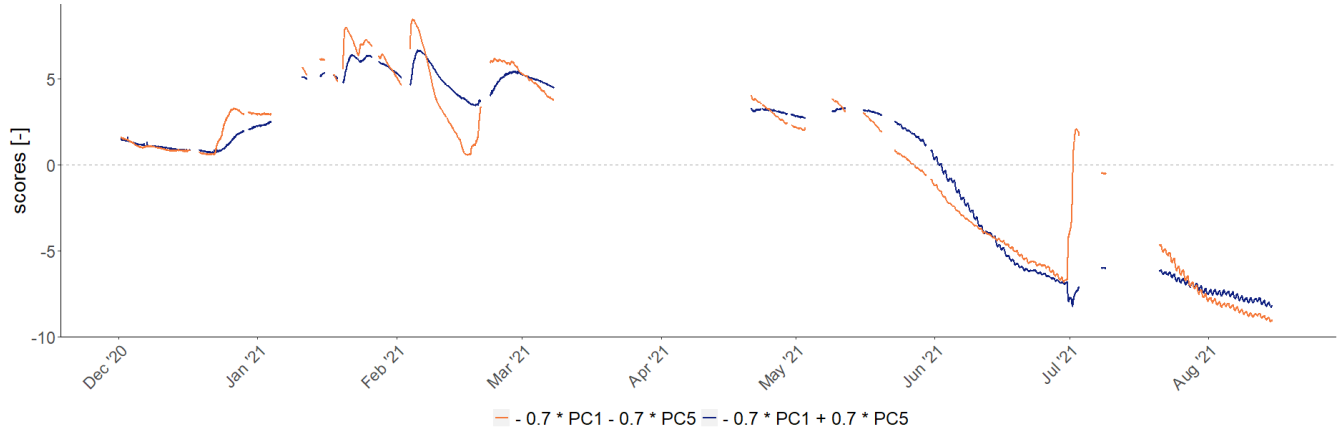

485

Figure 10: Effect of the fifth principal component on modification of the general mean behaviour which is presented by the first principal component.

Table 1: Overview of crop rotation, sand content down to 0.25m depth and weed control of analyzed patches.

Patch ID	Crop in winter season	Crop in growing season	Treatment	Sand content (in 1 m buffer zone around sensors) [%]	Weed control

https://doi.org/10.5194/egusphere-2023-1115
Preprint. Discussion started: 29 June 2023

81	Winter barley		A	78.3	conventional
89	Winter rye		A	80.5	conventional
95	Winter oats		A	80.7	conventional
115	Winter oats		A	80.6	reduced
90	Fallow	Lupine	B	80.6	conventional
110	Fallow	Lupine	B	80.3	reduced
51	Phacelia	Maize	C	80.8	reduced
102	Phacelia	Maize	C	80.6	conventional
12	Phacelia	Soy	C	78.5	reduced
66	Phacelia	Soy	C	77.9	conventional
96	Phacelia	Sunflower	C	80.6	conventional
105	Phacelia	Sunflower	C	80.5	reduced

490

Table 2: Overview of NDVI, surface temperature, both taken on May 31, 2021, and slope at the locations of analysed sensors.

Crop	Patch ID	Sensor Position	NDVI [-]	Surface Temperature [°C]	Slope [°]
Barley	81	West	0.93	20.57	2.01
Barley	81	East	0.93	20.43	1.94
Rye	89	West	0.85	22.39	1.74
Rye	89	East	0.82	24.95	1.67
Oats	95	East	0.83	27.25	1.36
Oats	95	West	0.85	27.85	1.15
Oats	115	West	0.88	23.70	1.28
Oats	115	East	0.84	25.12	0.43
Sunflower	96	West	0.20	33.76	0.59
Sunflower	96	East	0.20	34.70	0.69
Sunflower	105	West	0.65	29.79	1.04
Sunflower	105	East	0.34	34.53	1.00
Lupine	90	West	0.71	26.31	1.40
Lupine	90	East	0.72	24.96	1.27
Lupine	110	West	0.73	26.98	1.88
Lupine	110	East	0.65	26.76	2.50

https://doi.org/10.5194/egusphere-2023-1115
Preprint. Discussion started: 29 June 2023

Maize	51	West	0.20	35.44	0.82
Maize	51	East	0.27	35.29	0.93
Maize	102	West	0.19	37.88	0.88
Maize	102	East	0.18	38.03	0.90
Soy	12	West	0.18	34.87	1.71
Soy	12	East	0.16	34.44	1.11
Soy	66	West	0.15	35.09	2.40
Soy	66	East	0.15	34.39	2.13

Table 3: Pearson correlation coefficients between drone imagery products taken on May 31, 2021, and loadings of sensors in all depths or at single depths, respectively, on the second principal component. All correlations are highly significant ($p<0.01$).

	Sensors in all depths	**0.3 m**	**0.6 m**	**0.9 m**
Surface temperature	-0.853	-0.881	-0.909	-0.916
NDVI	0.887	0.9278	0.934	0.940

495

Table 4: Principal components 1 to 5.

	PC1	**PC2**	**PC3**	**PC4**	**PC5**
Eigenvalue	46.25	10.89	2.60	1.43	1.06
Proportion of variance [%]	72.27	17.01	4.06	2.23	1.65
Proportion of variance (cumulative)[%]	72.27	89.28	93.34	95.57	97.22
Interpretation	Mean behaviour	Winter vs. summer crops	Subsoil texture	Soil organic carbon	Damping of the input signal
Prevailing driver	weather	crop	soil	crop and soil	soil